

## Detecting clandestine tunnels using near-surface seismic techniques

Steven D. Sloan<sup>1</sup>, Shelby L. Peterie<sup>2</sup>, Richard D. Miller<sup>2</sup>, Julian Ivanov<sup>2</sup>,  
J. Tyler Schwenk<sup>1</sup>, and Jason R. McKenna<sup>3</sup>

### ABSTRACT

Geophysical detection of clandestine tunnels is a complex problem that has met with limited success. Multiple methods have been applied, spanning several decades, but a reliable solution has yet to be found. We evaluated shallow seismic data collected at a tunnel test site representative of geologic settings found along the southwestern U.S. border. Our results demonstrated the capability of using P-wave diffraction and surface-wave backscatter techniques to detect a purpose-built subterranean tunnel. Near-surface seismic data were also collected at multiple sites in Afghanistan to detect and locate subsurface anomalies, including data collected over the escape tunnel discovered in 2011 at the Sarposa Prison in Kandahar, Afghanistan, which allowed more than 480 prisoners to escape, and data from another shallow tunnel recently discovered at an undisclosed location. The final example from Afghanistan was the first time surface-based geophysical methods have detected a tunnel whose presence and location was not previously known. Seismic results directly led to the discovery of the tunnel. Interpreted tunnel locations for all examples were within less than 2 m of the actual location. Seismic surface-wave backscatter and body-wave diffraction methods showed promise for efficient data acquisition and processing for locating purposefully hidden tunnels within unconsolidated sediments.

### INTRODUCTION

Covert subterranean tunnels have been used for thousands of years with applications ranging from perimeter infiltration to more modern applications of drug smuggling. Most historical examples

are related to military applications, such as tunneling into enemy territory to mount a surprise attack. There have been multiple instances in the last century, including tunnels constructed beneath no-man's-land in Flanders, Belgium, during World War I, prison camp escape tunnels during World War II, the Cu Chi tunnels in Vietnam during the 1960s, and cross-border tunnels beneath the Korean Demilitarized Zone (DMZ) separating North Korea and South Korea from the 1970s to the 1990s. Four tunnels have been discovered beneath the Korean DMZ between 1974 and 1990, ranging in depth from approximately 1 to 350 m beneath the surface.

More modern examples include more than 170 drug-smuggling tunnels identified along the U.S.-Mexico border since 1990, tunnels between Egypt and Gaza that circumvent import/export restrictions, and tunnels from Gaza into Israel used to carry out tactical strikes. More than 30 tunnels were reported to have been located in the recent Israel-Gaza conflict in the summer of 2014. The conflicts in Iraq and Afghanistan have also produced cases of clandestine tunneling. In 2005, a tunnel was discovered at a military prison in Iraq that was 4.6 m deep and 109 m long (Fainaru and Shadid, 2005). A similar incident occurred in 2011 near Kandahar, Afghanistan, in which a reported 488 prisoners escaped from the Sarposa Prison, which is the largest prison in southern Afghanistan (Shah and Rubin, 2011). The tunnel took approximately five months to construct, running more than 300 m long and 1 m wide with electricity and ventilation throughout.

There are numerous examples in the literature of shallow seismic methods applied to void detection in general and tunnel detection using reflection (Branham and Steeples, 1988; Dobecki, 1988; Inazaki et al., 2005; Llopis et al., 2005; Sloan et al., 2010), refraction (Belfer et al., 1998; Llopis et al., 2005; Hickey et al., 2009; Riddle et al., 2010; Sloan et al., 2013), surface waves (Sloan et al., 2010; Schwenk et al., 2014), diffraction (Belfer et al., 1998; Landa and Keydar, 1998; Walters et al., 2009; Sloan et al., 2010; Peterie and Miller, 2015), borehole (Rechtien et al., 1995), and passive

Manuscript received by the Editor 10 November 2014; revised manuscript received 2 April 2015; published online 3 August 2015.

<sup>1</sup>XRI Geophysics, LLC, Vicksburg, Mississippi, USA. E-mail: steve.sloan@xrigeo.com; tyler.schwenk@xrigeo.com.

<sup>2</sup>Kansas Geological Survey, Lawrence, Kansas, USA. E-mail: speterie@kgs.ku.edu; rmiller@kgs.ku.edu; jivanov@kgs.ku.edu.

<sup>3</sup>Formerly United States Army Engineer Research & Development Center, Vicksburg, Mississippi, USA; presently 4QTRS Holdings, LLC, Vicksburg, Mississippi, USA. E-mail: jason.mckenna@4qtrs.net.

© 2015 Society of Exploration Geophysicists. All rights reserved.

methods (Tucker et al., 2007). Seismic techniques intuitively make sense based on the large contrast in material properties and seismic velocities between an air-filled cavity and the surrounding geologic medium. Although theory and models suggest this to be a straightforward problem, this has rarely proven to be true in real-world applications. Seismic methods have shown promise; however, they are also sensitive to elevated ambient noise levels and the subsequent decreased signal-to-noise ratio (S/N). Noise sources may include natural sources, such as wind or rain; anthropogenic sources, such as vehicle traffic, industrial noise, power lines, or air traffic; or geologic noise including boulders, stratigraphic pinch-outs, sand or clay lenses, etc.

The paper presented here highlights several shallow tunnels that have been encountered, including the Sarposa Prison escape tunnel and another tunnel at an undisclosed location that has been confirmed by excavation, which appears to be the first successful detection and confirmation of a previously unknown tunnel using surface-based geophysical methods, based on a review of the current refereed literature.

The methods described here use diffracted P-waves and backscattered surface waves (Figure 1). Seismic diffractions can occur as a result of subsurface pointlike objects, such as tunnels, pipes, mine workings, boulders, etc., that act as secondary energy radiation points and produce hyperbolic seismic signatures. Backscattered surface waves occur as a result of forward-propagating surface waves meeting a lateral velocity/density boundary that scatters a portion of the energy back toward the source. Diffractions and backscattered surface waves are a product of changes in seismic velocity and/or density, and both are sensitive to anomalies much smaller than the associated wavelength (Landa and Keydar, 1998; Sloan

et al., 2010). The backscattered and diffracted energy lend themselves to enhancement processing due to their unique and distinguishable characteristics that are different from other types of seismic responses. Diffractions and surface waves are considered to be noise in conventional seismic reflection processing with measures taken to eliminate or severely attenuate them. Typical reflection processing schemes seek to enhance reflected energy while minimizing the contribution of other wave types. Diffraction- and backscatter-focused processing are similar to reflection processing in that regard — diffracted or backscattered waves are emphasized at the expense of all other energy, including reflections. As noted by Berkovitch et al. (2009) and Landa and Keydar (1998), diffractions tend to be degraded, lost, or masked during the stacking and/or migration process due to weaker amplitudes compared with reflections and the inability of conventional moveout corrections to accurately approximate diffraction traveltimes. Landa and Keydar (1998) provide a good example comparing the differences between a migrated time section and a diffraction section containing a small-scale anomaly. The distinct contrast between material properties, such as density and velocity, of an air-filled void and the surrounding geologic medium, combined with the sensitivity to small features, make these techniques practical choices in the search for clandestine tunnels.

## METHODS

### Body-wave diffraction

The use of diffracted body waves to detect and localize small-scale subsurface heterogeneities has been presented by others (Landa et al., 1987; Kanasewich and Phadke, 1988; Landa and Keydar, 1998; Berkovitch et al., 2009; Peterie and Miller, 2015). All processed diffraction section examples presented in this article were processed using a scheme described by Peterie and Miller (2015) for mode-converted diffractions, with the notable exception that the algorithm used here focuses on P-wave diffractions. The processing flow was designed to enhance and focus diffractions, resulting in a 2D cross section that highlights subsurface sources of diffracted energy at the expense of other seismic information, such as reflections or surface waves.

Field records are corrected using a diffraction moveout velocity, assuming that each receiver potentially overlies a subsurface anomaly, and stacked. The resulting gathers, referred to as apex-enhanced shot gathers, are then sorted into common receiver gathers. A moveout correction is again applied assuming that an anomaly is positioned below the corresponding receiver location. The moveout-corrected common receiver gathers are subsequently stacked (one trace per receiver station) and displayed in a 2D cross section (Peterie and Miller, 2015). Moveout velocities are chosen based on the observable diffractions in field files, or by using first arrivals to approximate an average velocity for the near surface. The latter is more likely to be used in

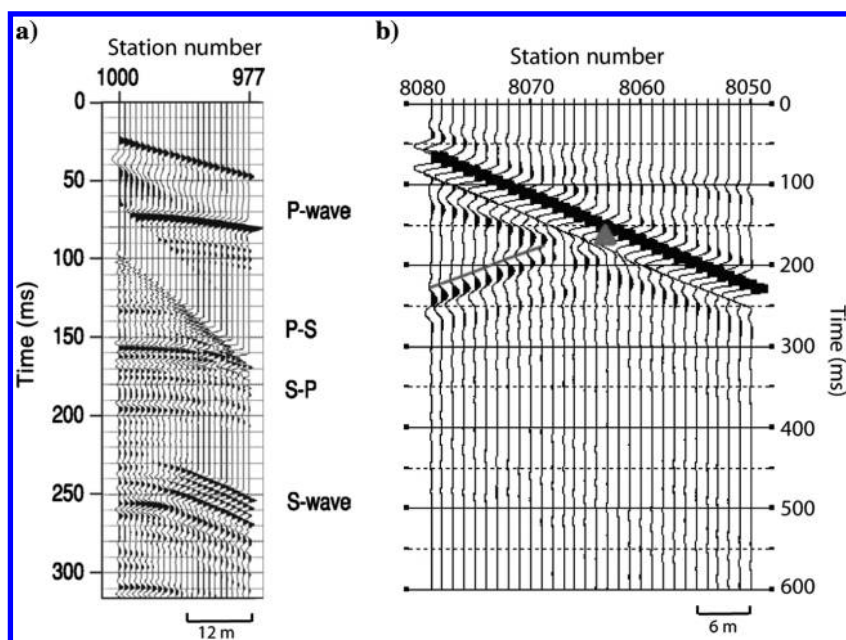


Figure 1. Synthetic shot gather examples of (a) body-wave diffractions and (b) backscattered surface waves. The shot gather on the left illustrates different modes (P, P-S, S-P, and S) and was generated using a homogeneous half space with  $V_P = 1000$  m/s,  $V_S = 300$  m/s, and an air-filled tunnel located underneath station 1000 at a depth of 30 m. The shot gather on the right was calculated using  $V_P = 475$  m/s,  $V_S = 230$  m/s, and an air-filled tunnel measuring 1.4 m wide by 2 m tall at a depth of 4.5 m.

cases in which the presence of an anomaly, and its depth, is unknown. In those cases, a range of velocities may be necessary to focus on a range of possible target depths.

The 2D diffraction section is qualitatively interpreted by identifying features that have higher amplitudes, relative to background levels, in which diffracted energy has been enhanced and constructively summed. It is important to note that the interpretation of a single line is nonunique because many types of subsurface features, natural and man made, can produce diffractions, e.g., boulders, stratigraphic pinch-outs, clay or sand lenses, or infrastructure such as sewer, water, or gas lines, etc. Determining the source of a given amplitude anomaly on a single cross section is difficult at best; however, by acquiring multiple parallel lines, locally isolated anomalies, such as a boulder, may be differentiated from linear features, such as a tunnel or mine adit, more confidently.

### Backscatter analysis of surface waves

The backscatter analysis of surface waves (BASWs) method aims to exploit backward propagating energy stemming from a subsurface anomaly (Sloan et al., 2010). The first step after defining the acquisition geometry and any required trace or record editing is to apply a user-defined  $f$ - $k$  filter to the field files to remove forward-propagating surface-wave energy. The resulting output yields enhanced backscatter energy, if present, from subsurface anomalies. Frequency-variant linear moveout (FV-LMO) (Park et al., 2002) corrections are then applied to the shot records using surface-wave velocities estimated from dispersion curves. After the FV-LMO-correction, residual forward-propagating energy remaining after the initial  $f$ - $k$  filter is shifted to time zero. Backscatter energy appears as the highest amplitude linear events sloping in the opposite direction as the forward energy. The FV-LMO corrected shot gathers are then sorted by receiver and stacked into a common receiver stack. Stacking enhances backscattered energy by constructively summing the backscattered signal originating from coincident station locations and attenuating other events.

High-amplitude, coherent dipping events are interpreted on the 2D BASW section. The station number in which the sloping backscatter event(s) cross time zero indicates the lateral location of the anomaly. A coherent event on the processed section suggests that a subsurface anomaly is present and provides an estimated lateral location on the surface; however, any correlation between the depth and/or size of the anomaly with the BASW section signature has not been observed to this point.

## FIELD EXAMPLES

### Example 1: Tunnel test site

Data were collected at a tunnel test site in southern Arizona representative of a dry desert environment similar to those found along the southwestern U.S. border. The site is composed of unconsolidated sand, silt, and clay, based on the drilling information from nearby boreholes. Soils mostly consist of loose to dense clayey sands and hard sandy clays. There is no groundwater within the upper 90 m at the site. The tunnel roof is 9.1 m (30 ft) deep. It is 1.5 m tall and 1.2 m wide and structurally supported by wooden shoring with fully enclosed walls, roof, and floor (Figure 2). The tunnel was constructed using tools and methods similar to those of actual tunnels that have been investigated along the U.S.-Mexico

border. Most importantly, the overburden above the tunnel has not been disturbed, as would be the case for an actual illicit tunnel, so any detectable seismic signatures can be attributed to the presence of the tunnel itself or its related effects and not related to the emplacement method, such as trenching and backfilling with disturbed soil. Cultural noise at the site is extremely low because the site is isolated far from cities or busy roads. Conditions are as ideal as one could ask for to collect seismic data, with wind, subsurface heterogeneity, and personnel movement as the main influences on data quality.

Data were acquired using an accelerated weight drop source and a 24-station land streamer that included 4.5- and 40-Hz vertical-component geophones at 1.22-m spacing pulled by a tow vehicle. Five shots were acquired and vertically stacked for each source location. Data were recorded by Geometrics Geode seismographs with 24-bit A/D conversion, 2-s trace lengths, and a 0.5-ms sampling interval. The offset between the source and nearest receiver was 36.6 m. Data were collected using a constant-offset roll-along style geometry with a source interval of 2.44 m. The array was advanced two stations for each source location, reaching a maximum fold of 12 at full coverage. Station locations were recorded using a real-time kinematic global positioning system.

The surface at the site was flat with dry, loose sediments and small patches of relatively short vegetation (small shrubs and cacti). Survey paths were chosen based on the distance from the vertical shaft and to minimize the amount of vegetation along the line, although it was impossible to avoid all plants. Line lengths measured approximately 140 m and were oriented perpendicular to the long axis of the tunnel. The 40- and 4.5-Hz geophones are used to emphasize different portions of the wavefield. Data from the former are used for the body-wave diffraction processing due to its

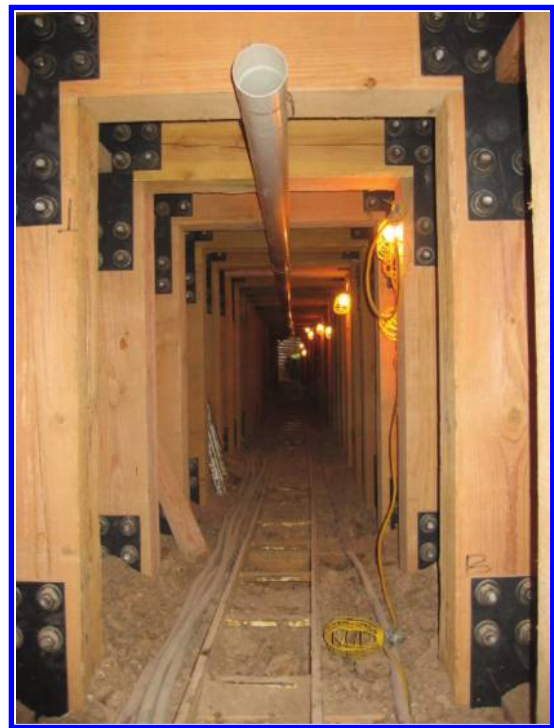


Figure 2. Picture of the inside of the test tunnel displaying wood shoring, rail tracks, ventilation pipe, and electric lighting.

higher frequency content, whereas data from the latter emphasize the lower frequency surface waves and are used in the BASW method. Hence, a single pass with the weight drop and land streamer results in two different data sets that exploit the body waves and surface waves. All data are displayed with the source and land streamer moving from lower to higher station numbers.

Line 1 was collected 40 m from the vertical access shaft, and line 2 was collected 30 m from the shaft (Figure 3). Lines were offset to avoid interference with the vertical shaft that could be misinterpreted as signatures from the tunnel. Data from line 1 are displayed

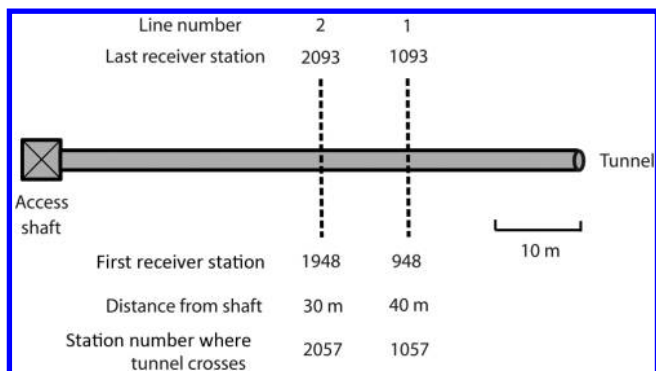


Figure 3. Diagram illustrating the layout of the seismic lines relative to the tunnel in example number 1. The depth to the roof of the tunnel is 9.1 m.

in Figure 4, including a shot gather highlighting a diffraction before processing (Figure 4a), the processed diffraction section (Figure 4b), the processed BASW section displayed in instantaneous amplitude (Figure 4c), and a shot gather indicating backscattered surface waves (Figure 4d). The shot gather in Figure 4a was collected using 40-Hz geophones and is shown with a 60-Hz low-cut filter and an  $f$ - $k$  filter to remove sloping events from 610 to 1035 m/s for display purposes to enhance the diffraction marked by the curved red line. The shot gather in Figure 4d was acquired using 4.5-Hz geophones and has had no processing applied. Backscattered energy is highlighted by the sloping red lines. The diffraction section in Figure 4b shows a high-amplitude anomaly at station 1057 that is higher than the background levels. A two-way traveltime of approximately 30 ms to the top of the anomaly, combined with a diffraction moveout velocity of 670 m/s, yields an estimated depth of 10 m, which is within 10% of the known target depth of 9.1 m. The backscattered surface-wave plot for line 1 shows a coherent, high-amplitude linear event that is interpreted to intersect  $t_0$  at station 1058. The tunnel is located at station number 1057 for line 1 (Figure 3).

Data from line 2 are displayed in a similar fashion in Figure 5a–5d. The shot gather in Figure 5a is displayed with a 100-Hz low-cut filter and a 610–1035 m/s  $f$ - $k$  filter. The diffraction section in Figure 5b shows a similar high-amplitude event to that in Figure 4b, located at station 2056. A two-way traveltime of approximately 28 ms, corresponds to an estimated depth of 9.4 m, which is within 3% of the known target depth. The backscattered surface-wave plot for line 2 also shows a coherent, high-amplitude event at station

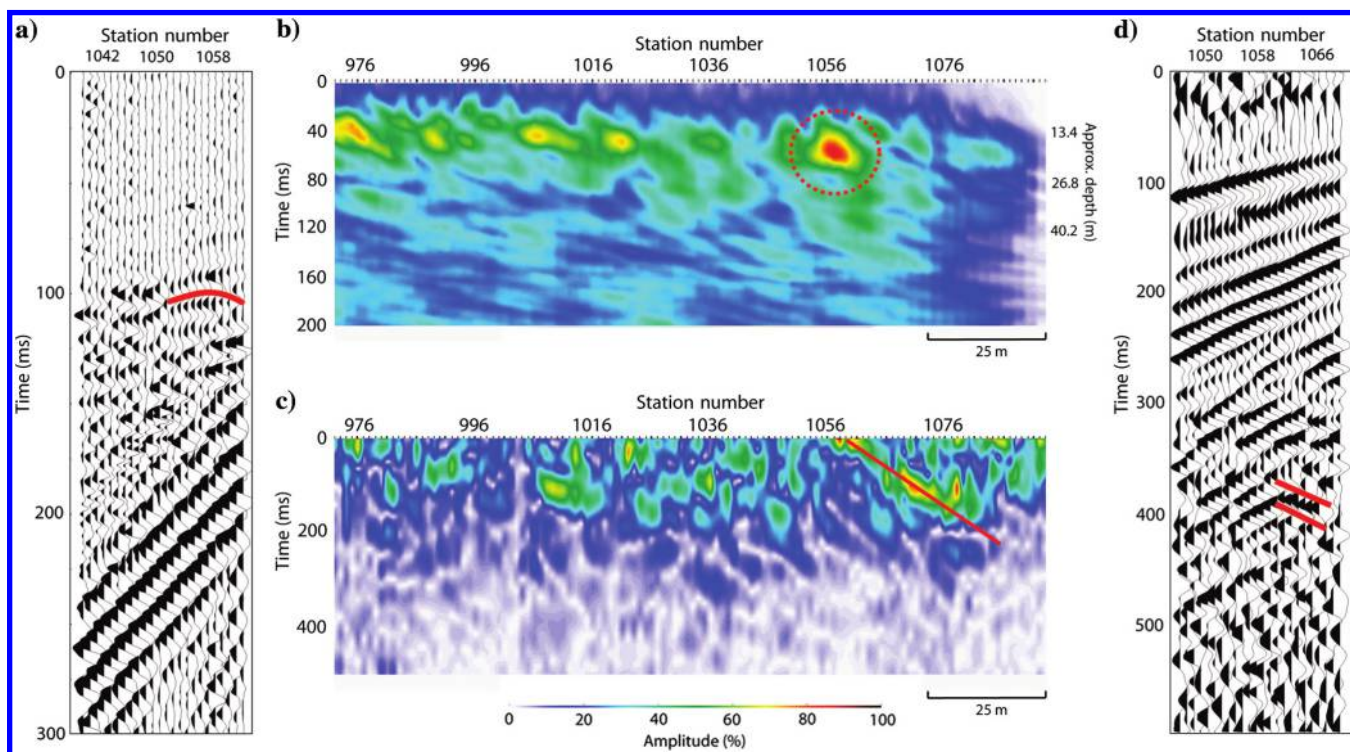


Figure 4. Data plots for line 1 in example 1: (a) shot gather acquired with 40-Hz geophones and a diffraction marked by the curved red line, (b) processed diffraction section with the interpreted tunnel anomaly marked by the red dashed circle, (c) processed BASW section displayed in instantaneous amplitude with the interpreted tunnel location indicated by the intersection of the red line with  $t_0$ , and (d) shot gather collected with 4.5-Hz geophones and backscatter highlighted by sloping red lines prior to processing. The shot gather in panel (a) is displayed with a 610–1035 m/s  $f$ - $k$  filter and 60-Hz low-cut filter for display purposes to emphasize the diffraction. The depth to the roof of the tunnel is 9.1 m.

2056 that is coincident with the location of the diffraction anomaly. The tunnel location for line 2 is station number 2057. The average  $V_P$  and  $V_S$  were 670 and 320 m/s, respectively, for the upper 10 m at the site.

The diffraction sections do exhibit other high-amplitude events besides those corresponding with the tunnel location; however, they do not display the same geometry. Signatures from the tunnel at this site consistently appear as relatively circular, high-amplitude events. This is to be expected because the source is a pointlike object in the subsurface and would appear as a point in the diffraction section using processing parameters perfectly matched to subsurface properties. Much like reflection processing, the selection of an incorrect moveout velocity will degrade the final processed section, leading to smeared or lower amplitude signatures, or their complete absence due to destructive interference during stacking. The other anomalies have not been confirmed by excavation, but may be resultant of geologic features, such as clay lenses, which have been observed in other data collected at the site, or source-generated noise that has not been completely removed by the stacking process. The lack of backscatter anomalies in the same vicinity suggests the latter is more likely. These events tend to be either lower in amplitude or elongated in shape relative to the tunnel signature, which aids interpretation of the plots and reduces the number of false positives at this site where both methods produced anomalies at coincident locations.

The BASW sections from this site tend to contain few signatures that match those from the known feature: high-amplitude, moderately sloping, coherent events. As with all geophysical methods,

those presented here can also suffer from nonuniqueness with similar signatures produced by geologic anomalies. However, the multimethod combination of the backscatter and diffraction techniques constrains our interpretation and increases confidence in the independently processed data sets.

Surface-wave data were also investigated using the multichannel analysis of surface waves (MASW) technique (Xia et al., 1999). However, a combination of higher mode surface waves obscuring the fundamental mode, acquisition parameters, and a velocity increase near the depth of interest resulted in our inability to confidently identify the tunnel using the MASW method at this site.

### Example 2: Sarposia Prison escape tunnel

A 1-m wide by 1-m tall tunnel was discovered at the Sarposia Prison near Kandahar, Afghanistan, in 2011. The tunnel was more than 300 m long and approximately 4 m deep, with brackets built into the walls to hold electrical lighting, ventilation along its entire length, and timber shoring (Figure 6). Seismic data were collected over the escape tunnel soon after its discovery and processed blindly by remotely located personnel without prior knowledge of its specific location. The site is located on the western side of Kandahar, situated east of the Arghandab River, north of the Rigestan Desert, and at the base of the Koh-e Baba mountains. The near-surface geology of the site is composed of unconsolidated alluvial gravels, sands, and clays.

Seismic data were collected using the same equipment and methods used at the tunnel test site described in example 1. The offset between the source and nearest receiver was 24.4 m. Data were col-

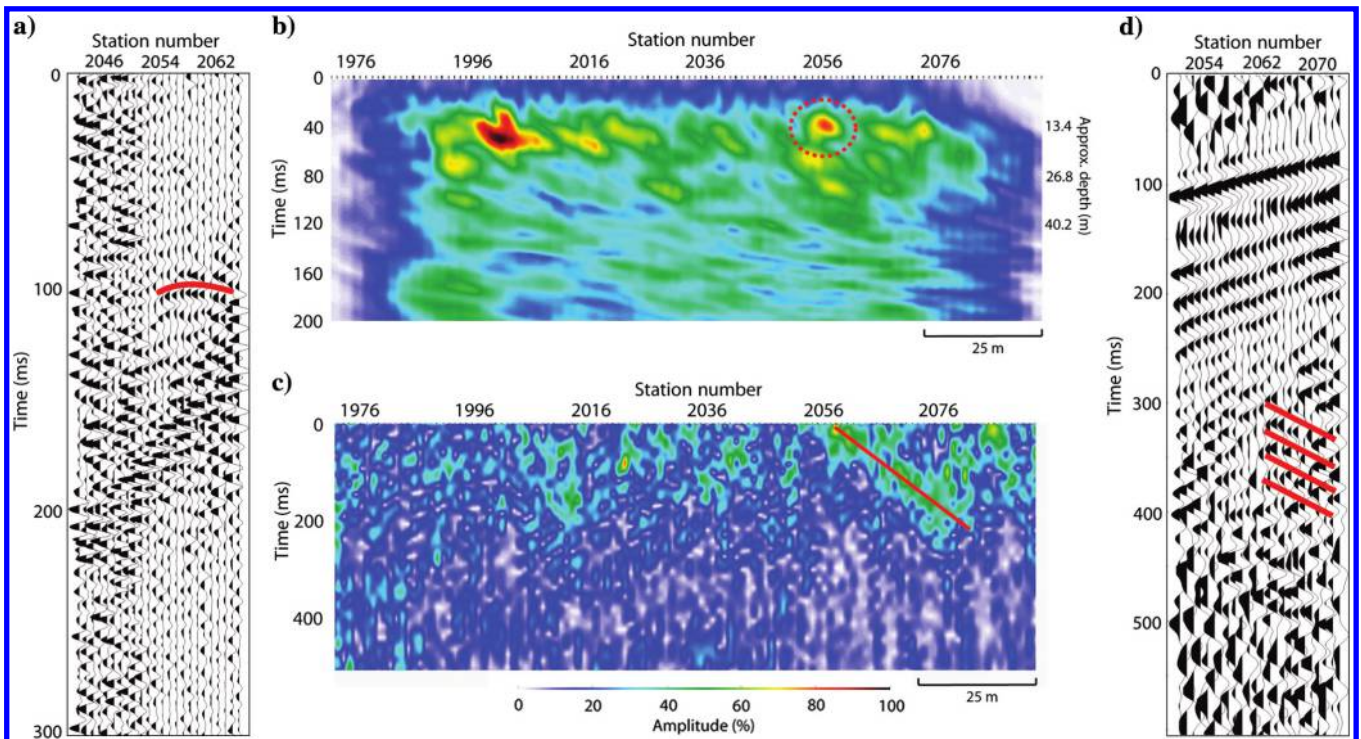


Figure 5. Data plots for line 2 in example 1: (a) shot gather acquired with 40-Hz geophones and a diffraction marked by the curved red line, (b) processed diffraction section with the interpreted tunnel anomaly marked by the red dashed circle, (c) processed BASW section displayed in instantaneous amplitude with the interpreted tunnel location indicated by the intersection of the red line with  $t_0$ , and (d) shot gather collected with 4.5-Hz geophones and backscatter highlighted by sloping red lines prior to processing. The shot gather in panel (a) is displayed with a 610–1035 m/s  $f$ - $k$  filter and 100-Hz low-cut filter for display purposes to emphasize the diffraction.

lected along a dry unimproved road. Due to space limitations, only a single line could be collected. The total length of the line was approximately 83 m. The orientation of the tunnel relative to the survey line was less than  $20^\circ$  from perpendicular.

Figure 7a–7d shows data collected over the known tunnel discovered at Sarposa Prison in 2011. Figure 7a and 7d is a common source gather with the interpreted diffraction and backscatter events, respectively. Figure 7b and 7c displays the processed diffraction and BASW sections, respectively. The interpreted apex of the diffraction



Figure 6. Photograph of the inside of the tunnel discovered at the Sarposa Prison in southern Afghanistan in 2011.

is at station 3981 in the shot gather, and the diffraction section shows a high-amplitude event at station 3980 (Figure 7b). A difference of plus-or-minus one station is not surprising considering the nature of the event in a common-shot gather — a low-amplitude signature surrounded by high-amplitude noise — and the difficulty in separating diffractions from ground roll and first arrivals. It is also likely that a subsurface feature will be located somewhere between two geophones, as opposed to perfectly aligned with a single station, increasing the difficulty of interpreting the apex.

The interpreted zero crossing of the backscatter anomaly is at station 3979. Although the station numbers of the interpreted anomalies do not match exactly, they are within a two-station spread (2.4 m), which is consistent with results from the tunnel test site in example 1. The estimated depth of the tunnel based on two-way traveltimes and the diffraction moveout velocity (625 m/s) is approximately 4.5 m deep. The actual depth to the roof of the tunnel, located at station number 3980, is approximately 3.9 m. The average  $V_P$  and  $V_S$  were 625 and 330 m/s, respectively, for the upper 5 m at the site. The tunnel was eventually filled in with cement slurry to prevent future use and to ensure the integrity of an overlying roadway, which is a main thoroughfare in that area. The water table was not encountered in the upper 5 m.

### Example 3: Clandestine tunnel in Afghanistan

A second tunnel was detected and confirmed in Afghanistan; however, its location has been withheld due to security concerns.

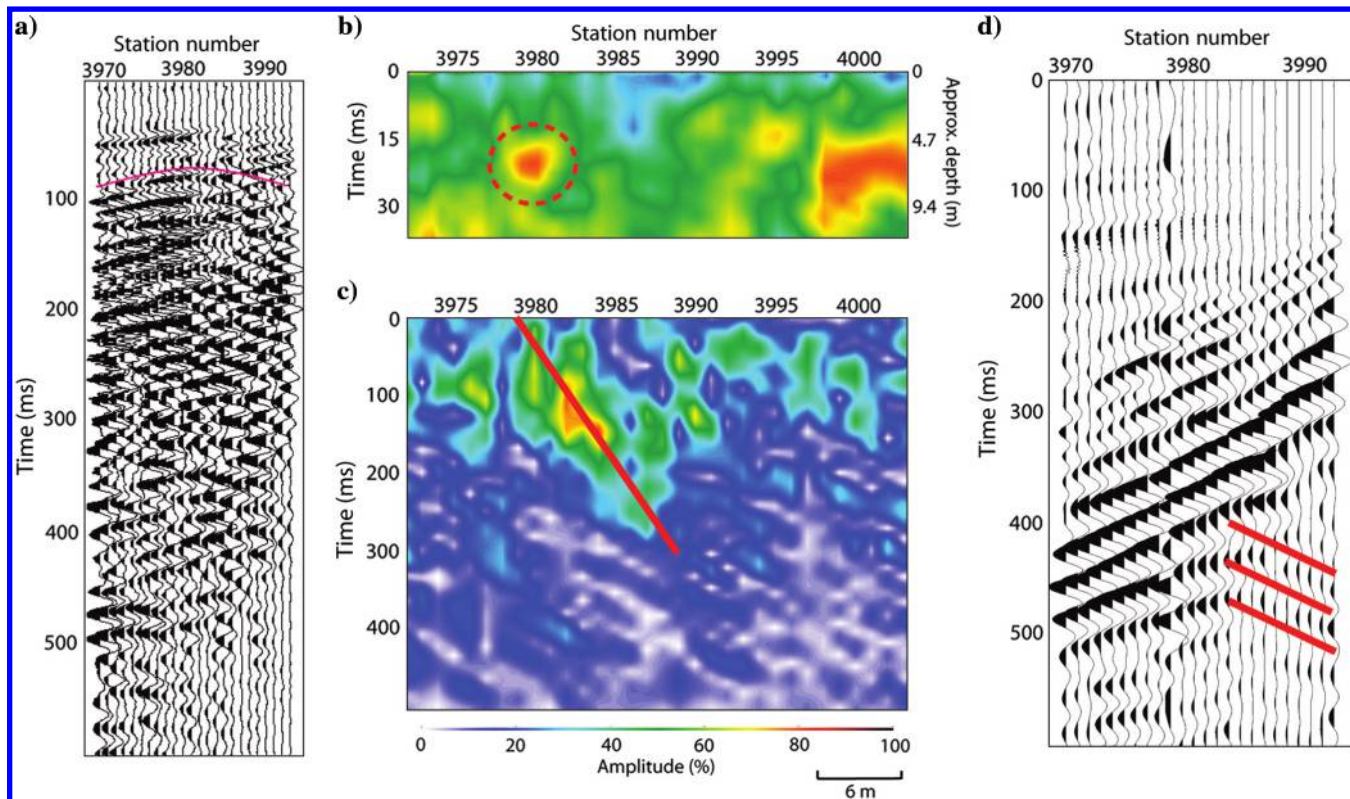


Figure 7. Seismic data collected over the Sarposa Prison escape tunnel in example 2: (a) shot gather acquired with 40-Hz geophones and a diffraction marked by the curved red line, (b) processed diffraction section with the interpreted tunnel anomaly marked by the red dashed circle, (c) processed BASW section displayed in instantaneous amplitude with the interpreted tunnel location indicated by the intersection of the red line with  $t_0$ , and (d) shot gather collected with 4.5-Hz geophones and backscatter highlighted by sloping red lines prior to processing.

The presence of this tunnel was completely unknown at the time of the survey and was excavated based on the information provided by the seismic analysis. Near-surface materials at the site mainly consisted of unconsolidated clays and sands. The water table was not present within the excavated depth of 7 m. Data were collected along a loose gravel road using the same acquisition parameters as listed in example 2. The line was 73 m long. The area immediately adjacent to the gravel appeared to have been reworked by heavy equipment, such as an excavator or bulldozer, but no information about the site was available at the time of the survey.

Overall, the data appear to be of lower quality (scattered energy and incoherency) compared with the data in example 2, despite being acquired under similar conditions. Backscattered and diffracting events are more difficult to pick in shot gathers and are less coherent. Despite this, there is an anomaly present in the diffraction section, interpreted to be at station 3995 (Figure 8b). The two-way traveltimes and estimated velocity (565 m/s) yields an approximate depth of 7 m. The sloping event in the BASW plot (Figure 8c) is interpreted to cross  $t_0$  at station 3994, within one station (1.2 m) of the diffractor location. The location to dig was selected as the difference between the two, and the target was confirmed by excavation to be within 1 m of the interpreted location, between stations 3993 and 3994. The measured depth of the tunnel was 6.2 m. The average

$V_P$  and  $V_S$  were 565 and 285 m/s, respectively, for the upper 7 m at the site.

The diffraction anomaly in this example is notably lower in amplitude relative to the rest of the section, especially in comparison with the previous two examples, and it may not have stood out in a longer line. One potential cause may be suboptimal processing parameters, such as an incorrect moveout velocity; however, the results did not appreciably improve by increasing or decreasing the velocity. Another reason may be the disturbance of the near-surface materials if they had been recently reworked as noted above. This would essentially create a distorted layer that the downgoing and upgoing waves would have to propagate through, possibly lowering the overall S/N. Surface waves are the dominant energy in typical shot gathers; it is not altogether surprising that the BASW section shows a strong response whereas the diffraction anomaly is more subtle.

## DISCUSSION

The methods discussed show promise for detecting illicit subsurface tunnels that have been historically notoriously difficult to identify. Data acquisition and processing can be accomplished quickly and efficiently, relative to conventional seismic techniques. In this

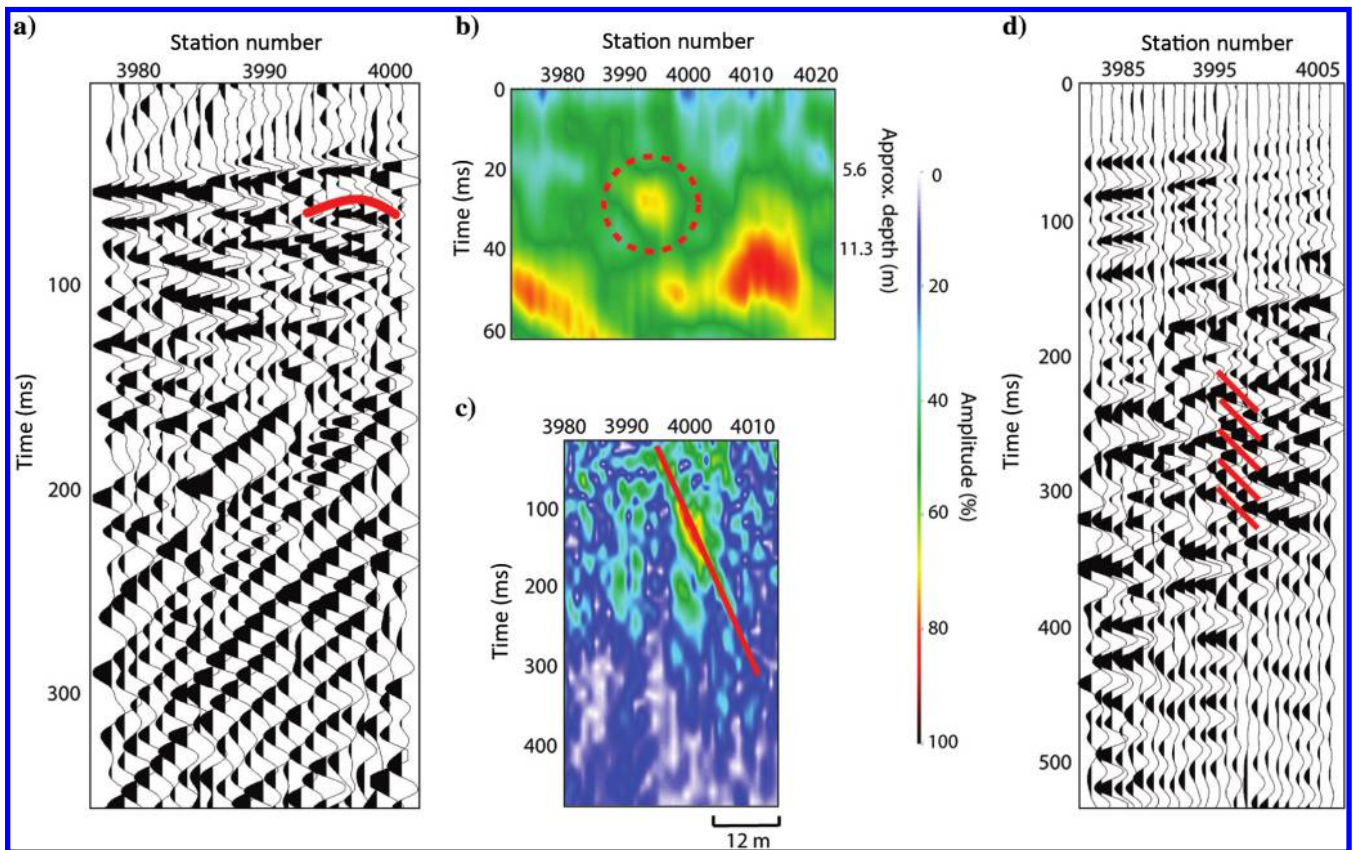


Figure 8. Seismic data collected over the recently discovered tunnel in Afghanistan in example 3: (a) shot gather acquired with 40-Hz geophones and a diffraction marked by the curved red line, (b) processed diffraction section with the interpreted tunnel anomaly marked by the red dashed circle, (c) processed BASW section displayed in instantaneous amplitude with the interpreted tunnel location indicated by the intersection of the red line with  $t_0$ , and (d) shot gather collected with 4.5-Hz geophones and backscatter highlighted by sloping red lines prior to processing. The shot gather in panel (d) is shown with an  $f$ - $k$  filter of 183–305 m/s for display purposes to remove a portion of the forward-propagating surface waves and highlight the backscattered events.

type of geologic setting, our results suggest that a shallow subterranean void can be detected using near-surface seismic diffractions and backscattered surface waves. The real strength of the methods described here is the application of two different techniques focusing on different portions of the wavefield. This serves to constrain interpretations and increase confidence in the results when there are coincident anomalies, but it also helps to avoid missing a potential target when one particular method does not perform as well. Example 3 is a good example, in which the diffraction section contained a relatively weak anomaly, whereas the BASW anomaly was strong. Although the identification of diffractions in the field records support the BASW interpretation, it was the surface-wave anomaly that keyed in processors to focus on that area.

There were no false positives in the examples presented here that resulted in unnecessary excavation largely because there were no other coincident anomalies in the diffraction and BASW sections that warranted digging. The overall length of a survey area is likely also a factor. Longer survey lines will inevitably produce more anomalies that require further investigation, some of which may turn out to be processing artifacts or naturally occurring geologic features. Certain geologic settings will also be more conducive to false positives, such as a fluvial setting that might contain paleochannels, clay or sand lenses, gravel bars, etc., that could produce similar signatures.

Diffractions can be difficult to identify in shot gathers due to their relatively low amplitude, proximity to first arrivals, and abundance of high-amplitude surface waves, but interpreting the lateral location is straightforward using either the apex in shot gathers or by amplitude in the processed section. Depth estimation is largely dependent on the processing parameters selected, especially the moveout correction velocity, and the interpreter making the actual picks. As such, it should be considered as an approximation and can vary from one processor/interpreter to another. Backscattered surface waves were easier to discern in field records, but interpreting the position of the anomaly on a BASW section is more subjective. The  $t_0$  crossing can easily shift several stations one way or the other depending on the interpretation of the linear features. As with shallow seismic reflection methods, interpretation of the processed sections should be augmented and supported by shot gathers. Verifying the presence of a diffraction and/or backscatter event in field records at the same location as interpreted anomalies is prudent to avoid misinterpretations of processing artifacts.

Potential pitfalls to be mindful of include targets that are oblique to the survey line and mode-converted diffractions. According to [Peterie and Miller \(2015\)](#), diffractions from a tunnel oblique to the survey line produce an asymmetric signature that will be shifted from the actual location. The authors suggest acquiring a minimum of three lines — two lines that are coincident but shot in opposite directions to determine the lateral shift correction and a third line offset from the first two to determine the tunnel azimuth. Although not encountered in the three examples here, mode-converted diffractions, such as P-S, can also lead to misinterpretation or targets missed altogether ([Peterie and Miller, 2015](#)). Mode-converted diffractions exhibit a polarity reversal at the apex, which would lead to destructive summing after correcting for moveout and stacking. The difference in velocity for the downgoing and upgoing legs must also be accounted for to accurately estimate depth. The oblique angles and mode conversion can be accounted for during processing and interpretation, but must first be recognized by a cognizant geophysi-

clist, emphasizing the need for good quality control procedures at various stages of processing.

There is currently no silver bullet or one-size-fits-all solution to this complex problem; the use of multiple methods increases the chance of success and improves confidence in interpretations by having multiple coincident data sets to cross-reference “hits” and reduce the number of false positives. Although seismic methods are presented here, other geophysical techniques may work as well, or better, in some geologic settings and should not be discounted. The use of additional methods that are sensitive to other physical properties might also be useful in constraining interpretations and further reducing misinterpretations. These techniques worked well in each of the examples presented, which were all applied in similar environments (dry unconsolidated materials). Small personnel footprints and relatively quick data collection rates are necessary for military and/or law enforcement applications. Those requirements, combined with positive performance and the practicality of using an accelerated weight drop source and towed land streamer for acquisition, are what led to the selection of seismic methods to be used in this setting.

## CONCLUSIONS

Tunnel detection continues to be a challenging geophysical problem; however, the methods discussed show promise in being capable of detecting and locating subsurface anomalies of interest. The examples presented demonstrate that diffractions and backscattered surface waves can be used effectively to search for covert tunnels in this type of geologic setting characterized by dry unconsolidated materials. Data acquisition and processing can be accomplished relatively quickly and efficiently. Practitioners should be aware of potential pitfalls to avoid misinterpretations or missing targets. Interpreted anomalies should be correlated with events in field records to avoid false positives and misinterpretation of processing artifacts.

Identifying small-scale subterranean features, such as a tunnel, has proven to be difficult under ideal conditions. It becomes much more so when looking for such subtle signatures in an operational environment in which noise sources are plentiful and data acquisition parameters may be compromised due to mission requirements, logistical constraints, and the notion that sometimes some data, albeit noisy, are better than no data at all. Despite these challenges, we were successful in detecting and locating a known tunnel that had been recently discovered, and a completely unknown target that was subsequently confirmed by excavation. Both data sets were processed without any guarantee of the presence of a tunnel, let alone knowledge of their locations.

## ACKNOWLEDGMENTS

We would like to thank O. Metheny and M. Davey for their hard work in the field and countless members of the U.S. military for support overseas. We also thank the associate editor and the anonymous reviewers for their constructive comments and suggestions that greatly improved the paper.

## REFERENCES

Belfer, I., I. Bruner, S. Keydar, A. Kravtsov, and E. Landa, 1998, Detection of shallow objects using refracted and diffracted seismic waves: *Journal*

- of Applied Geophysics, **38**, 155–168, doi: [10.1016/S0926-9851\(97\)00025-6](https://doi.org/10.1016/S0926-9851(97)00025-6).
- Berkovitch, A., I. Belfer, Y. Hassin, and E. Landa, 2009, Diffraction imaging by multifocusing: *Geophysics*, **74**, no. 6, WCA75–WCA81, doi: [10.1190/1.3198210](https://doi.org/10.1190/1.3198210).
- Branham, K. L., and D. W. Steeples, 1988, Cavity detection using high-resolution seismic reflection methods: *Mining Engineering*, **40**, 115–119.
- Dobecki, T. L., 1988, A rapid seismic technique for detecting subsurface voids and unmapped mine workings: Proceedings of the 1st EEGS Symposium on the Application of Geophysics to Engineering and Environmental Problems, Environmental and Engineering Geophysical Society, 666–690, doi: [10.4133/1.2921819](https://doi.org/10.4133/1.2921819).
- Fainaru, S., and A. Shadid, 2005, In Iraq jail, resistance goes underground: Washington Post, A01.
- Hickey, C. J., D. R. Schmitt, J. M. Sabatier, and G. Riddle, 2009, Seismic measurements for detecting underground high-contrast voids: Proceedings of the 22nd EEGS Symposium on the Application of Geophysics to Engineering and Environmental Problems, 929–936.
- Inazaki, T., S. Kawamura, O. Tazawa, Y. Yamanaka, and N. Kano, 2005, Near-surface cavity detection by high-resolution seismic reflection methods using short-spacing type land streamer: Proceedings of the Symposium on the Application of Geophysics to Engineering and Environmental Problems, 959–970.
- Kanasewich, E. R., and S. M. Phadke, 1988, Imaging discontinuities on seismic sections: *Geophysics*, **53**, 334–345, doi: [10.1190/1.1442467](https://doi.org/10.1190/1.1442467).
- Landa, E., and S. Keydar, 1998, Seismic monitoring of diffraction images for detection of local heterogeneities: *Geophysics*, **63**, 1093–1100, doi: [10.1190/1.1444387](https://doi.org/10.1190/1.1444387).
- Landa, E., V. Shtivelman, and B. Gelchinsky, 1987, A method for detection of diffracted waves on common-offset sections: *Geophysical Prospecting*, **35**, 359–373, doi: [10.1111/j.1365-2478.1987.tb00823.x](https://doi.org/10.1111/j.1365-2478.1987.tb00823.x).
- Llopis, J. L., J. B. Dunbar, L. D. Wakeley, and M. K. Corcoran, 2005, Tunnel detection along the southwest U.S. border: Proceedings of the Symposium on the Application of Geophysics to Engineering and Environmental Problems, 430–443.
- Park, C. B., R. D. Miller, and J. Ivanov, 2002, Filtering surface waves: Proceedings of the Symposium on the Application of Geophysics to Engineering and Environmental Problems, 1–10.
- Peterie, S. L., and R. D. Miller, 2015, Near surface scattering phenomena and implications for tunnel detection: *Interpretation*, **3**, no. 1, SF43–SF54, doi: [10.1190/INT-2014-0088.1](https://doi.org/10.1190/INT-2014-0088.1).
- Rechtien, R. D., R. J. Greenfield, and R. F. Ballard, 1995, Tunnel signature prediction for a cross-borehole seismic survey: *Geophysics*, **60**, 76–86, doi: [10.1190/1.1443765](https://doi.org/10.1190/1.1443765).
- Riddle, G. I., C. J. Hickey, and D. R. Schmitt, 2010, Subsurface tunnel detection using electrical resistivity tomography and seismic refraction tomography: A case study: Proceedings of the 23rd EEGS Symposium on the Application of Geophysics to Engineering and Environmental Problems, 552–562.
- Schwenk, J. T., S. D. Sloan, R. D. Miller, and J. Ivanov, 2014, Correlation of the backscatter analysis of surface waves method (BASW) for anomaly detection: 84th Annual International Meeting, SEG, Expanded Abstracts, 2029–2035.
- Shah, T., and A. J. Rubin, 2011, Taliban breach Afghan prison; Hundreds free: *The New York Times*, A1.
- Sloan, S. D., J. J. Nolan, S. W. Broadfoot, J. R. McKenna, and O. M. Metheny, 2013, Using near-surface seismic refraction tomography and multichannel analysis of surface waves to detect shallow tunnels: A feasibility study: *Journal of Applied Geophysics*, **99**, 60–65, doi: [10.1016/j.jappgeo.2013.10.004](https://doi.org/10.1016/j.jappgeo.2013.10.004).
- Sloan, S. D., S. L. Peterie, J. Ivanov, R. D. Miller, and J. R. McKenna, 2010, Void detection using near-surface seismic methods, *in* R. D. Miller, J. D. Bradford, and K. Holliger, eds., *Advances in near-surface seismology and ground-penetrating radar*: SEG Geophysical Developments Series 15, 201–218.
- Tucker, R. E., J. R. McKenna, M. H. McKenna, and M. S. Mattice, 2007, Detecting underground penetration attempts at secure facilities: *Engineer*, **37**, 31–34.
- Walters, S. L., R. D. Miller, D. W. Steeples, J. Xia, and C. Zeng, 2009, Detecting tunnels and underground facilities using diffracted P-waves: Proceedings of the Symposium on the Application of Geophysics to Engineering and Environmental Problems, 937–942.
- Xia, J., R. D. Miller, and C. B. Park, 1999, Estimation of near-surface shear-wave velocity by inversion of Rayleigh wave: *Geophysics*, **64**, 691–700, doi: [10.1190/1.1444578](https://doi.org/10.1190/1.1444578).